Geometry and Numerics of CMC Surfaces with Radial Metrics

Gabriel dos Reis

INSTITUT NATIONAL DE RECHERCHE EN INFORMATIQUE ET EN AUTOMATIQUE

Geometry and Numerics of CMC Surfaces with Radial Metrics

Gabriel Dos Reis

N° 4763

Mars 2003

THÈME 2

ISSN 0249-6399 ISRN INRIA/RR--4763--FR+ENG

Geometry and Numerics of CMC Surfaces with Radial Metrics

Gabriel Dos Reis

Thème 2 — Génie logiciel
et calcul symbolique
Projet GALAAD

Rapport de recherche n° 4763 — Mars 2003 — 26 pages

Abstract: Thsi paper investigates the geometry of non-zero constant mean curvature surfaces with radial metric, putting an emphasis on the link between the Hopf differential and the extrinsic geometry. New asymptotic estimations of the metrics are given at the umbilical point and at infinity. The last section proposes an algorithm for numerical constructions.

Key-words: CMC surfaces, Hopf differential, ODE, Gauss–Mainardi–Codazzi equations, numerical integration, visualization.

Unité de recherche INRIA Sophia Antipolis
2004, route des Lucioles, BP 93, 06902 Sophia Antipolis Cedex (France)
Téléphone : +33 4 92 38 77 77 — Télécopie : +33 4 92 38 77 65

Géométrie et aspects numériques des surfaces CMC à métriques radiales

Résumé : Ce papier étudie en détail la géométrie des surfaces à courbure moyenne constante non nulle avec une métrique radiale, en mettant en lumière le rôle la différentielle de Hopf dans la géométrie extinsèque. Nous démontrons en particulier des estimations nouvelles de la métrique près du point ombilic et à l'infini. Enfin, nous proposons un algorithme de construction numérique de ces surfaces.

Mots-clés : Surfaces CMC, différentielle de Hopf, ÉDO, équations de Gauss–Mainardi–Codazzi, intégration numérique, visualisation.

1 Introduction

Shapes study and description are the main subject of the branch of Differential Geometry concerned with the theory of sub-manifolds. According to the fundamental theorem of that field, the bulk of the work is the analysis of the well-known Codazzi–Mainardi and Gauss–Codazzi equations. Right now, there is no known effective methods to tackle the general problem of shape description based on knowledge about the Gauss and Codazzi partial differential relations — although some preliminary work have been done by É. Cartan using his method of moving frame. In practice, the shapes under study in specific contexts exhibit some particular geometry. That additional information often proves to simplify the equations investigations. In this article, we conduct that project for surfaces with constant mean curvature with a 1-parameter group of intrinsic symmetries, ending up with an effective symbolic and numerical algorithm for the construction of such surfaces.

The interest in surfaces with constant mean curvature originates from isoperimetric problems and variational problems. Classical geometers knew that a smooth surface, with minimal area, that spans a given contour ought to have opposite principal curvatures everywhere — such surfaces are called minimal surfaces. Analogously, it can be shown that a closed surface, with minimal area, that encloses a given volume has a non zero constant mean curvature everywhere. The French geometer Gaston Darboux [5] pointed out that the rôles played by Gaussian curvature in Geometry and mean curvature in Physics give the greatest importance to the construction and study of surfaces on which either of those curvature functions are constant.

The construction and the study of constant mean curvature surfaces have prompted geometers to develop various representations. For minimal surfaces, the theory is relatively well understood thanks to works by K. Weierstrass and A. Enneper who reduced the problem to an issue in the theory of Complex Analysis and Algebraic Geometry, exploiting the holomorphic character of the associated Gauss maps. For non-zero constant mean curvature surfaces (*CMC surfaces* for short), the situation is dramatically less understood because their Gauss maps are no longer holomorphic: They are merely harmonic.

It should be emphasized that the value of explicit (numerical) construction of such surfaces should not be underestimated. Apart from the CMC surfaces of revolution — discovered and classified by Ch. Delaunay [6] more than a century and half ago — and the trivial examples of round spheres and cylinders, the theory of CMC surfaces remained stalled since the 1950s until mid 1980 when H. Wente [15] positively answered a famous question of H. Hopf by abstractly constructing a CMC torus. It is U. Abresch [1] who, intrigued by the appearance of the numerical constructions based on Wente's paper, was able to geometrically characterize Wente's tori. That characterization then incitated U. Pinkall and I. Sterling [12], A.I. Bobenko [3] to apply soliton theory to the study of CMC tori. In all those works, the numerical simulations have played fundamental rôles in suggesting several possible geometric facts that were eventually proved true.

Recently, J. Dorfmeister and his coworkers [7] have derived a device (called DPW method) that theoretically constructs all CMC immersions of simply connected domains; their methods heavily uses abstract theories of loop group factorizations, starting with holomorphic potentials. However, the factorizations steps — constructions happening in an infinite-dimensional Lie group — still not well understood seriously hinder the derivation of geometric properties from the defining holomorphic potentials. Among the rare geometric invariants one can read off from the DPW recipe, appears the Hopf differential. We have settled to understand how that quadratic differential influences the external geometry of a CMC surface. In the present paper we carry out that project for CMC surfaces with internal rotational symmetry.

This paper investigates the geometry, algorithmic and numerics of constant mean curvature surfaces with radial metrics discovered by Brian Smyth [13]. These surfaces have been studied by various geometers [13, 14, 4]. The paper of Timmreck et *al.* [14] attempted to prove their properness, but it contains a serious gap. The paper of Bobenko [4] investigated the cone bounded-ness of these surfaces through the theory of Painlevé equations but it didn't address the properness of the immersions. In this article, we give a complete proof of the properness of Smyth surfaces, hence providing the first rigorous demonstration of that fact. By taking a global approach (as opposed to [14] and [4]), we are able to give a correct proof, initiate a frame-

work for investigating more general Smyth-like surfaces [8, 9], give new asymptotics of the metric (therefore asymptotic behavior of both the intrinsic and extrinsic geometries). We also set up an algorithm, based on the Gauss, Weingarten and Gauss–Codazzi equations, for numerical construction of Smyth surfaces. The pictures shown in this paper were obtained by variations on that algorithm.

This paper is organized as follows. Section §2 recalls basic facts from the classical theory of surfaces and settles notations; in particular it derives an analytic representation (which we call Bonnet representation) of sufficiently smooth immersions in the Euclidean 3-dimensional space $\mathcal{E}^3$ in terms of their underlying Riemann surfaces, metrics, mean curvature functions and Hopf differentials. Section §3 reduces the problem of constructing constant mean curvature immersions of the planes with intrinsic rotational symmetry to that of solving a singular Differential Equation. In section §4 we prove the existence and uniqueness of the solutions (with the obvious initial conditions) to the equation obtained in the preceding section; that proves the existence and uniqueness — up to rigid motions — of Smyth surfaces. The section §5 gives an asymptotic expansion of the metric near the umbilical point; this result appears to be new. The section §6 is devoted to carrying out various asymptotic expansions at infinity, with a corollary that Smyth surfaces are properly immersed. In section §8 we study the geometry of the "legs" of Smyth surfaces. Finally, in section §9 we derive an algorithm for numerical construction of Smyth surfaces; that section illustrates how a combination of symbolic and numerical methods can lead to effective and powerful tools of visualization and investigation in Differential Geometry.

2 Basic facts from classic theory of surfaces

Throughout this article, a *surface* is defined to be a smooth immersion of a topological space in the Euclidean 3-dimensional space. To every surface $\boldsymbol{f} : \mathrm{Dom}\,(\boldsymbol{f}) \longrightarrow \mathcal{E}^3$, there corresponds the so-called first fundamental form defined by

$$\mathrm{I}_{\boldsymbol{f}} = \langle \mathrm{d}\boldsymbol{f},\, \mathrm{d}\boldsymbol{f} \rangle$$

on the tangent bundle $\mathrm{T}\,\boldsymbol{f}$. A local coordinate system $(x,\,y)$ is said isothermic for $\boldsymbol{f}$ if the following relations hold:

$$\mathrm{I}_{\boldsymbol{f}}\left(\frac{\boldsymbol{\partial}}{\boldsymbol{\partial x}},\frac{\boldsymbol{\partial}}{\boldsymbol{\partial x}}\right)=\mathrm{e}^{2\omega}=\mathrm{I}_{\boldsymbol{f}}\left(\frac{\boldsymbol{\partial}}{\boldsymbol{\partial y}},\frac{\boldsymbol{\partial}}{\boldsymbol{\partial y}}\right)\quad\text{and}\quad\mathrm{I}_{\boldsymbol{f}}\left(\frac{\boldsymbol{\partial}}{\boldsymbol{\partial x}},\frac{\boldsymbol{\partial}}{\boldsymbol{\partial y}}\right)=0.$$

It is known that any twice-differentiable surface admits a local isothermic coordinate around all points (see [11]). Furthermore, if $\mathrm{Dom}\,(\boldsymbol{f})$ is orientable then there exists an isothermic local coordinate system for $\boldsymbol{f}$. It follows that any orientable twice-differentiable surface possesses an underlying Riemann surface structure.

We define the Gauss map of an immersion $\boldsymbol{f}$ as the unit normal vector field along $\boldsymbol{f}$ according to the identities

$$\boldsymbol{N}=\boldsymbol{e}_x\times\boldsymbol{e}_y,\quad\text{where}\quad\boldsymbol{e}_x=\mathrm{e}^{-\omega}\,\frac{\partial\boldsymbol{f}}{\partial x},\quad\boldsymbol{e}_y=\mathrm{e}^{-\omega}\,\frac{\partial\boldsymbol{f}}{\partial y}.$$

The local deviation of $\boldsymbol{f}$ from its tangent plane is measured by the second fundamental form

$$\mathrm{II}_{\boldsymbol{f}}=-\left\langle\mathrm{d}\boldsymbol{f},\,\mathrm{d}\boldsymbol{N}\right\rangle.$$

This quadratic form is associated with the shape operator $\mathrm{A}_{\boldsymbol{f}}$ (or Weingarten map) relatively to the first fundamental form

$$\mathrm{I}_{\boldsymbol{f}}\left(\mathrm{A}_{\boldsymbol{f}}\left(\boldsymbol{U}\right),\boldsymbol{V}\right)=\mathrm{II}_{\boldsymbol{f}}\left(\boldsymbol{U},\boldsymbol{V}\right)=\mathrm{I}_{\boldsymbol{f}}\left(\boldsymbol{U},\,\mathrm{A}_{\boldsymbol{f}}\left(\boldsymbol{V}\right)\right).$$

The principal curvatures (resp. directions) of the surface $\boldsymbol{f}$ are the eigenvalues (resp. eigen-directions) of the shape operator. Moreover, the algebraic invariants

$$H_{\boldsymbol{f}}=\frac{1}{2}\,\mathrm{tr}\,\mathrm{A}_{\boldsymbol{f}}\quad\text{and}\quad K_{\boldsymbol{f}}=\det\mathrm{A}_{\boldsymbol{f}}$$

are actually geometric invariants and called the mean and Gaussian curvatures of the surface $\boldsymbol{f}$. The interested reader may consult [5] for further details.

If, in an isothermic local coordinate $(x,\,y)$, the second fundamental form is written

$$\mathrm{II}_{\boldsymbol{f}}=\lambda\mathrm{d}x^2+2\mu\mathrm{d}x\mathrm{d}y+\nu\mathrm{d}y^2,$$

then the second variations of the vector position $\boldsymbol{f}$ and the first variations of the normal field are respectively given by the Gauss equations

$$\left\{\begin{array}{l} \dfrac{\partial^2 \boldsymbol{f}}{\partial x^2} = \dfrac{\partial \omega}{\partial x}\dfrac{\partial \boldsymbol{f}}{\partial x} - \dfrac{\partial \omega}{\partial y}\dfrac{\partial \boldsymbol{f}}{\partial y} + \lambda \boldsymbol{N} \\ \dfrac{\partial^2 \boldsymbol{f}}{\partial x \partial y} = \dfrac{\partial \omega}{\partial y}\dfrac{\partial \boldsymbol{f}}{\partial x} + \dfrac{\partial \omega}{\partial x}\dfrac{\partial \boldsymbol{f}}{\partial y} + \mu \boldsymbol{N} \\ \dfrac{\partial^2 \boldsymbol{f}}{\partial y^2} = -\dfrac{\partial \omega}{\partial x}\dfrac{\partial \boldsymbol{f}}{\partial x} + \dfrac{\partial \omega}{\partial y}\dfrac{\partial \boldsymbol{f}}{\partial y} + \nu \boldsymbol{N} \end{array}\right. , \tag{1}$$

and the Weingarten equations

$$\left\{\begin{array}{l} \dfrac{\partial \boldsymbol{N}}{\partial x} = -\,\mathrm{e}^{-2\omega}\left(\lambda \dfrac{\partial \boldsymbol{f}}{\partial x} + \mu \dfrac{\partial \boldsymbol{f}}{\partial y}\right) \\ \dfrac{\partial \boldsymbol{N}}{\partial y} = -\,\mathrm{e}^{-2\omega}\left(\mu \dfrac{\partial \boldsymbol{f}}{\partial x} + \nu \dfrac{\partial \boldsymbol{f}}{\partial y}\right) \end{array}\right. . \tag{2}$$

For future reference, we will set up some general equations (following [8] which contains expanded details), using the complex coordinate $z = x + \imath y = \varrho\, \mathrm{e}^{\imath \vartheta}$ derived from an isothermal local coordinate $(x,\, y)$. Firstly, let us consider the complex-valued function Q defined by

$$Q\,(z) = \frac{\lambda - \nu}{2} - \imath \mu.$$

It is easily seen that the object $Q \mathrm{d}z^2$ is a quadratic differential on $\mathrm{Dom}\,(\boldsymbol{f})$ and that its zeros precisely correspond to the umbilical points of the surface $\boldsymbol{f}$. Secondly, a curve $t \mapsto z\,(t) \in \mathrm{Dom}\,(\boldsymbol{f})$ drawn on the surface $\boldsymbol{f}$ is a line of curvature if and only if it is a solution the differential equation

$$\mathrm{Im}\left[Q\,(z\,(t))\left(\frac{\mathrm{d}z}{\mathrm{d}t}\right)^2\right] = 0. \tag{3}$$

Thirdly, the geodesic curvature of the curve $\boldsymbol{f}\,(z\,(t))$ is given by the formula (see [8])

$$\kappa_g\,(t) = \mathrm{e}^{-\omega}\left(\kappa_z\,(t) + \frac{\partial \omega}{\partial n_z}\right), \tag{4}$$

where κ_z designates the curvature of the plane curve $z(t)$ and n_z its outer normal.

Finally, the compatibility conditions for the systems of partial differential relations (1) and (2) are respectively given by the Codazzi–Mainardi equations

$$\frac{\partial Q}{\partial \overline{z}} = \mathrm{e}^{2\omega}\,\frac{\partial H}{\partial z} \quad \text{and} \quad \frac{\partial \overline{Q}}{\partial z} = \mathrm{e}^{2\omega}\,\frac{\partial H}{\partial \overline{z}} \tag{5}$$

and the Gauss–Codazzi equation

$$\Delta\omega + H^2\,\mathrm{e}^{2\omega} - |Q|^2\,\mathrm{e}^{-2\omega} = 0. \tag{6}$$

That the first and second fundamental forms suffice to describe completely the local geometry of a surface is the content of Fundamental Theorem of the theory of surfaces:

Theorem 1 (O. Bonnet) *Given two real-valued functions ω, H and a quadratic differential $Q\mathrm{d}z^2$ defined on a Riemann surface $\mathcal{M}$, all subject to the differential relations* (5) *and* (6)*, there corresponds a unique immersion — up to rigid motions of $\mathcal{E}^3$ — of its universal cover $\boldsymbol{f} : \widetilde{M} \longrightarrow \mathcal{E}^3$ with fundamental forms*

$$\mathrm{I} = \mathrm{e}^{2\omega}\,|\mathrm{d}z|^2 \quad \textit{and} \quad \mathrm{II} = \frac{Q}{2}\mathrm{d}z^2 + H\,\mathrm{I} + \frac{\overline{Q}}{2}\mathrm{d}\overline{z}^2.$$

3 CMC surfaces with radial metrics

In a remarkable paper published in 1841, Ch. Delaunay [6] determined and classified all CMC surfaces of revolution. He identified the embedded (resp. immersed) ones as the roulette of ellipsis (resp. hyperbola). Nearly a century and a half later, B. Smyth [13] set the project to determine all complete CMC surfaces with a continuous group of intrinsic symmetries — the external rotational symmetry is not necessarily assumed. He came to the following conclusions:

1. To every natural number $n \in \mathbb{N}$ corresponds a 1-parameter family of complete, isometric conformal immersions $\boldsymbol{f}_n^{\vartheta} : \mathbb{C} \longrightarrow \mathcal{E}^3$ with mean curvature 1 of the plane such that the induced metric is invariant by

rotation through $0 \in \mathbb{C}$ corresponding to the (unique) umbilical point (of order n).

2. Any complete CMC immersion admitting a continuous 1-parameter group of intrinsic isometries is contained in the associated family of a Delaunay surface or of the above mentioned surface.

We will denote by $\mathbf{Sm}_n$ the surfaces discovered by B. Smyth [13]. The approach taken in this paper to study the geometry of the immersions $\mathbf{Sm}_n$ is fundamentally different from that of [13] since our main concerns are:

- the rôle played by the Hopf differential;
- algorithmic (numerical) construction of $\mathbf{Sm}_n$;
- properness of the immersions and what they look like.

We would like to emphasize that none of those points were addressed in B. Smyth's paper.

From the Codazzi–Mainardi equations (5), it is easily seen that the mean curvature function of a surface $\boldsymbol{f}$ is constant if and only if its Hopf differential is holomorphic. Therefore a simply connected CMC surface is completely determined — up to rigid motions — by a holomorphic quadratic differential $Q\mathrm{d}z^2$ and a function ω solution of the Gauss–Codazzi equation (6). It may be observed that if the pair $(\omega,\, Q)$ solves equation (6) then so does the pair $(\omega,\, \mathrm{e}^{it}\, Q)$ for $t \in \mathbb{R}$. Therefore, a constant mean curvature surface always pops up as part of a family of isometric immersions; that family is called the associated family. Furthermore, if we require the metric $\mathrm{I} = \mathrm{e}^{2\omega}\, |\mathrm{d}z|^2$ to have a rotational symmetry, then after an eventual translation, the function Q is monomial. It may be shown (see [8, Chapter 4]) that after a possible change of isothermal coordinate, the function Q may be written $Q\,(z) = Hz^n$, with $n \in \mathbb{N}$.

As noted at §2, the lines of curvature of a surface are the trajectories of its associated Hopf differential. For the Smyth surfaces, it is readily seen that the lines of greatest curvature are given by

$$\mathrm{Im}\left(z^{\frac{n+2}{2}}\right) = \mathrm{const} = \varrho^{\frac{n+2}{2}} \sin \frac{n+2}{2}\vartheta$$

whereas the lines of the smallest curvature are given by

$$\operatorname{Re}\left(z^{\frac{n+2}{2}}\right) = \text{const} = \varrho^{\frac{n+2}{2}} \cos\frac{n+2}{2}\vartheta.$$

Each foliation contains $(n+2)$ critical rays that meet at the umbilical point,

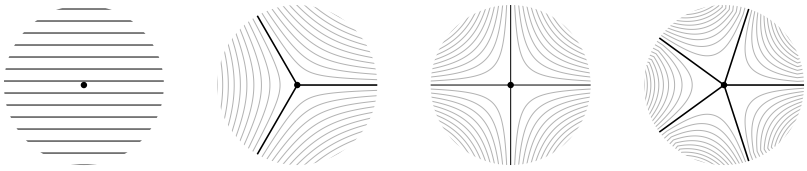

Figure 1: Horizontal trajectories of $z^n \mathrm{d}z^2$

the angle between two consecutive rays being $\pi/(n+2)$. This pattern is preserved by conformal parameterization. Before getting into the core details of determining the metrics of Smyth_n, let us remark that the quantity $H^2\,\mathrm{e}^{2\omega}$ is invariant by rigid motions and scaling transformations in $\mathcal{E}^3$. Therefore, we define

$$\sigma = H\,\mathrm{e}^{\omega(0)}\,.$$

We will see later that σ is the initial velocity of the geodesic emanating from the origin.

With the above data, the construction of complete CMC surfaces with an intrinsic rotational symmetry is essentially an exercise in integration of the singular differential equation (reduced form of the Gauss–Codazzi equation)

$$\frac{\mathrm{d}^2\omega}{\mathrm{d}\varrho^2} + \frac{1}{\varrho}\frac{\mathrm{d}\omega}{\mathrm{d}\varrho} + H^2\left(\mathrm{e}^{2\omega} - \varrho^{2n}\,\mathrm{e}^{-2\omega}\right) = 0. \tag{7}$$

with the natural initial conditions

$$\omega\,(0) = \ln\frac{\sigma}{H} \quad \text{and} \quad \left.\frac{\mathrm{d}\omega}{\mathrm{d}\varrho}\right|_{\varrho=0} = 0. \tag{8}$$

4 Existence and uniqueness

Since the differential equation (7) is singular at the origin, the theorem of Cauchy–Lipschitz is no longer directly applicable. However the theory developed by Baouendi and Goulaouic [2] ensures the existence and the uniqueness of a maximal solution ω_n defined on an interval $[0,\, \varepsilon_n[$, satisfying the initial condition (8). As a consequence, we get the existence of CMC immersions of $\mathcal{D}\,(O,\, \varepsilon_n)$ with intrinsic rotational symmetry. We want to prove that $\varepsilon_n = +\infty$. To that end, we define the following functions on $]0,\, \varepsilon_n[$

$$\upsilon_n(\varrho) = \omega_n\,(\varrho) - \frac{n}{2}\ln\varrho, \tag{9}$$

$$E_n\,(\varrho) = \frac{1}{2\varrho^n}\left(\frac{\mathrm{d}\upsilon_n}{\mathrm{d}\varrho}\right)^2 + 2H^2\sinh^2\upsilon_n. \tag{10}$$

The function E_n may be thought of as a reduced energy function. We observe:

Lemma 1 *The function E_n has a (finite) limit at ε_n.*

Proof. The change of dependent variable (9) transforms the differential equation (7) into

$$\frac{\mathrm{d}^2\upsilon_n}{\mathrm{d}\varrho^2} + \frac{1}{\varrho}\frac{\mathrm{d}\upsilon_n}{\mathrm{d}\varrho} + 4H^2\varrho^n\sinh\upsilon_n\cosh\upsilon_n = 0,$$

from which we conclude that

$$\frac{\mathrm{d}E_n}{\mathrm{d}\varrho} = -\frac{n+2}{2\varrho^{n+1}}\left(\frac{\mathrm{d}\upsilon_n}{\mathrm{d}\varrho}\right)^2. \tag{11}$$

So, the function E_n is decreasing; therefore, being non-negative, it has a limit at infinity. □

For future reference, we denote by $E_n\,(\infty)$ the value of the limit of E_n at infinity. We are now prepared to state:

Theorem 2 *The differential equation* (7) *has a unique solution defined on all $\mathbb{R}_+$ satisfying the initial conditions* (8).

Proof. This follows from the previous lemma and the following classical result in the theory of Differential Equations (see [10]):

> If the function $f(\varrho, u)$ is locally Hölderian in the first variable and locally Lipschitzian in the second variable and the function $u \in \mathscr{C}^2([0, \eta[)$ is a maximal solution of the differential equation
>
> $$\frac{\mathrm{d}^2 u}{\mathrm{d}\varrho^2} + \frac{1}{\varrho}\frac{\mathrm{d}u}{\mathrm{d}\varrho} + f(\varrho, u) = 0$$
> $$u(0) = 0 \quad \text{and} \quad \left.\frac{\mathrm{d}u}{\mathrm{d}\varrho}\right|_{\varrho=0} = 0,$$
>
> then either
>
> - $\eta = +\infty$; or else
> - there exists a real number $r > 0$ such that
>
> $$\overline{\lim_{\varrho \to r^-}} |u(\varrho)| = +\infty \quad \text{and} \quad \overline{\lim_{\varrho \to r^-}} \left|\frac{\mathrm{d}u}{\mathrm{d}\varrho}\right| = +\infty.$$

Let us assume that ε_n is finite; then, the relation (10) defining the reduced energy E_n and the lemma 1 imply that both v_n and $\mathrm{d}v_n/\mathrm{d}\varrho$ are bounded near ε, but then that contradicts the result quoted above. □

So, we have proved the existence of CMC immersions of the plane with intrinsic rotational symmetry. Their completeness will be proved later. It may be observed that when $n = 0$, then the trivial solution $\omega_0 \equiv 0$ is the only constant solution: It corresponds to the round cylinder of radius $1/2H$.

5 Asymptotics near the umbilical point

The behaviour of Smyth surfaces near the umbilical point has not received much attention in the literature. Here we prove the following result (which seems to be new):

Theorem 3 *Any solution ω_n of the equation* (7) *with the initial conditions* (8) *has the asymptotic expansion*

$$\omega_n(\varrho) = \ln \frac{\sigma}{H\left[1+\left(\frac{\sigma\varrho}{2}\right)^2\right]} + o\left(\varrho^{2n}\right) \tag{12}$$

near $\varrho = 0$.

Proof. We may remark that since ω_n is analytic and we are looking for its Taylor expansion up to order $2n$, the right hand side of the equation

$$\frac{\mathrm{d}^2\omega}{\mathrm{d}\varrho^2} + \frac{1}{\varrho}\frac{\mathrm{d}\omega}{\mathrm{d}\varrho} + H^2\,\mathrm{e}^{2\omega} = H^2\varrho^{2n}\,\mathrm{e}^{-2\omega}$$

may be safely neglected and the resulting equation — with the stated initial conditions — is that defining the function appearing in the right hand side of asymptotic expansion (12). □

We would like to point out that the metric

$$\mathrm{I}_\infty = \frac{\sigma^2}{H^2}\frac{|\mathrm{d}z|^2}{\left[1+\left(\frac{\sigma|z|}{2}\right)^2\right]^2}$$

is that of a round sphere, and since a CMC surface is uniquely determined by its metric, it appears that $\mathbf{Sm}_n$is asymptotic to a sphere at the origin, and that the accuracy improves as n gets high.

6 Asymptotics at infinity

A corollary of lemma 1 is the following estimations:

$$v_n(\varrho) = \mathcal{O}(1) \quad \text{and} \quad \frac{\mathrm{d}v_n}{\mathrm{d}\varrho} = \mathcal{O}\left(\varrho^{n/2}\right), \quad \varrho \to \infty. \tag{13}$$

We may conclude that for $n \geqslant 1$, the surfaces Smyth_n are complete. For the purpose of deriving better asymptotic behaviours, we may state

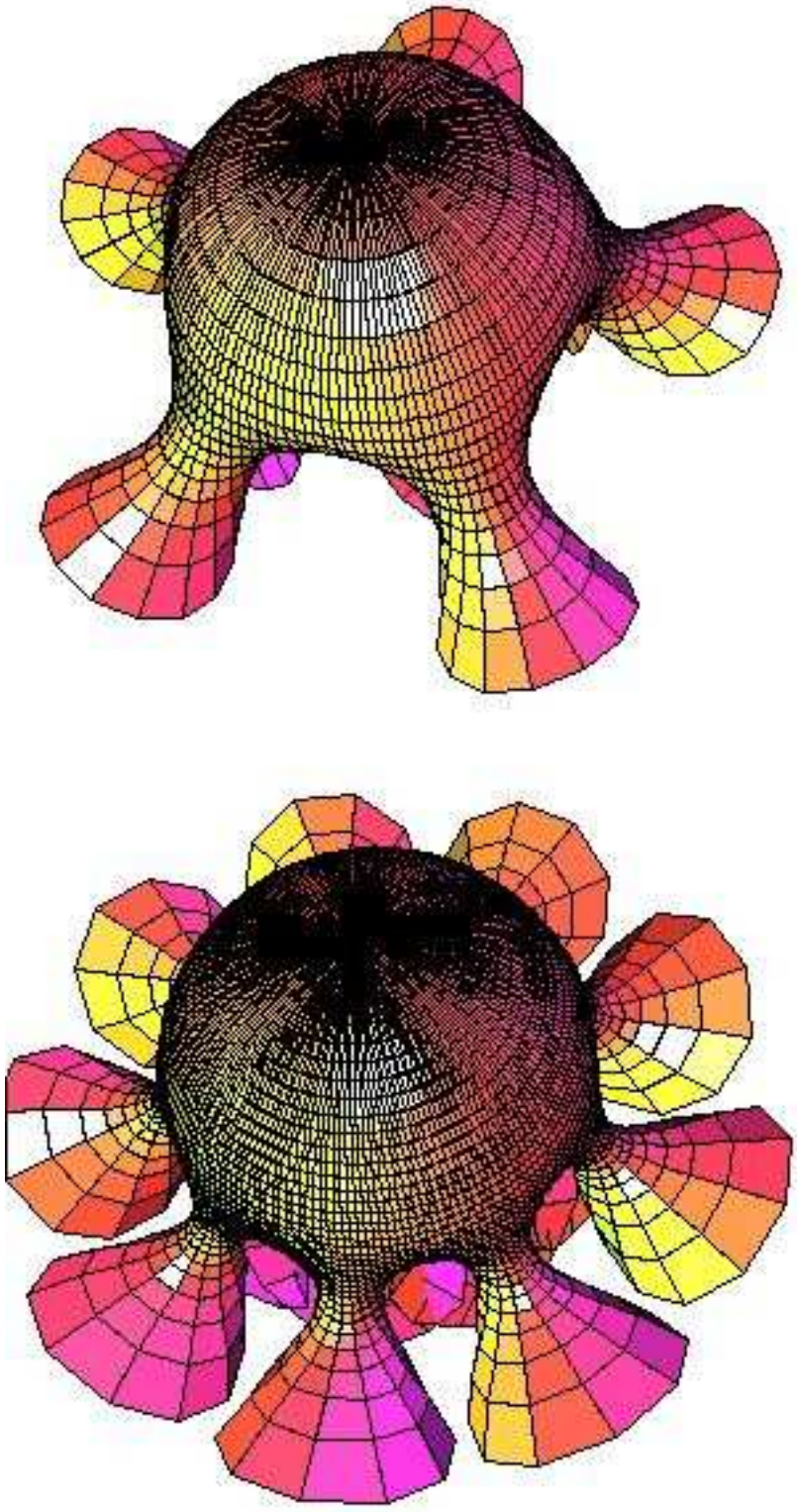

Figure 2: Smyth surfaces near the umbilic for $n = 3$ and $n = 7$

Lemma 2 *The function*

$$\varrho \mapsto \frac{1}{\varrho^{n+1}} \left(\frac{\mathrm{d}\upsilon_n}{\mathrm{d}\varrho} \right)^2$$

is integrable at infinity.

Proof. Indeed, according to the relation (11), we have

$$\int_{r_1}^{r_2} \frac{1}{\varrho^{n+1}} \left(\frac{\mathrm{d}\upsilon_n}{\mathrm{d}\varrho} \right)^2 \mathrm{d}\varrho = \frac{2}{n+2} \left(E_n\left(r_1\right) - E_n\left(r_2\right) \right).$$

The assertion claimed in the lemma is therefore equivalent to that of the existence of a limit for E_n at infinity; something lemma 1 already ensures. □

The next assertion we make is:

Lemma 3 *The function*

$$\varrho \mapsto \frac{\sinh^2 \upsilon_n}{\varrho}$$

is integrable at infinity.

Proof. Consider the quantity

$$V\left(r_1,\, r_2\right) = \int_{r_1}^{r_2} \frac{1}{\varrho^{n+1}} \left(\frac{\mathrm{d}\upsilon_n}{\mathrm{d}\varrho} \right)^2 \mathrm{d}\varrho.$$

An integration by parts yields

$$V\left(r_1,\, r_2\right) = \left[\frac{\upsilon_n}{\varrho^{n+1}} \frac{\mathrm{d}\upsilon_n}{\mathrm{d}\varrho} \right]_{r_1}^{r_2} + \int_{r_1}^{r_2} \left(\frac{n+2}{\varrho} \frac{\mathrm{d}\upsilon_n}{\mathrm{d}\varrho} + \frac{4H^2}{\varrho} \sinh \upsilon_n \cosh \upsilon_n \right) \upsilon_n \mathrm{d}\varrho.$$

However, the estimations (13) imply

$$\lim_{r_2 \to +\infty} \left[\frac{\upsilon_n}{\varrho^{n+1}} \frac{\mathrm{d}\upsilon_n}{\mathrm{d}\varrho} \right]_{r_1}^{r_2} = -\frac{\upsilon_n}{r^{n+1}} \frac{\mathrm{d}\upsilon_n}{\mathrm{d}r}.$$

The same estimations give

$$\frac{n+2}{\varrho^{n+2}} \frac{\mathrm{d}\upsilon_n}{\mathrm{d}\varrho} \upsilon_n = \mathcal{O}\left(\frac{1}{\varrho^2} \right),$$

thus the integral

$$\int_r^\infty \frac{n+2}{\varrho^{n+2}} \frac{\mathrm{d}\upsilon_n}{\mathrm{d}\varrho} \upsilon_n \mathrm{d}\varrho$$

is well-defined and has a finite value. Since lemma 2 implies that the quantity $V(r_1,\, r_2)$ has a limit as r_2 goes to infinity, one concludes the integrability of the function

$$\varrho \mapsto \frac{\upsilon_n}{\varrho} \sinh \upsilon_n \cosh \upsilon_n.$$

But then, the function υ_n being bounded at infinity — according to estimation (13) — one sees that the claim of the lemma follows at once. □

Now, it is obvious that according to the identity (10) and the two lemmas we just proved, we have established the following result:

Theorem 4 *The function $\varrho \mapsto E_n(\varrho)/\varrho$ is integrable at infinity.*

As a corollary, we have

$$E_n(\infty) = \lim_{\varrho\to\infty} E_n(\varrho) = 0 \tag{14}$$

$$\upsilon_n(\varrho) = o(1), \quad \frac{\mathrm{d}\upsilon_n}{\mathrm{d}\varrho} = o\left(\varrho^{n/2}\right) \quad \text{and} \quad \omega_n(\varrho) = \frac{n}{2}\ln\varrho + o(1). \tag{15}$$

We may observe that all Smyth surfaces corresponding to $n = 0$ have fundamental forms asymptotic to those of the round cylinder with radius $1/2H$.

For the purpose of obtaining further asymptotics, we will use a variation on the Prüfer method. To that end, it will be helpful to introduce the functions α_n and φ_n defined on $\mathbb{R}_+^*$ according to the relations

$$\alpha_n = \frac{1}{E_n}\frac{\mathrm{d}E_n}{\mathrm{d}\varrho}, \tag{16}$$

$$\frac{\mathrm{d}\upsilon_n}{\mathrm{d}\varrho} = -\sqrt{2\varrho^n E_n}\sin\varphi_n \quad \text{and} \quad \sqrt{2}H\sinh\upsilon_n = \sqrt{E_n}\cos\varphi_n. \tag{17}$$

Then, it follows by differentiation that

$$\alpha_n(\varrho) = -\frac{n+2}{\varrho}\sin^2\varphi_n \tag{18}$$

$$\frac{\mathrm{d}\varphi_n}{\mathrm{d}\varrho} = 2H\varrho^{n/2}\cosh\upsilon_n - \frac{n+2}{2\varrho}\sin(2\varphi_n). \tag{19}$$

Since we know that the function υ_n tends to zero at infinity, if follows from the above equality that the following estimation holds:

$$\frac{\mathrm{d}\varphi_n}{\mathrm{d}\varrho} \sim 2H\varrho^{n/2}, \quad \varrho \to \infty.$$

As a consequence we have the following lemma:

Lemma 4 *There exists real positive numbers A_n and B_n such that the function φ_n is a diffeomorphism from $[A_n, \infty[$ onto $[B_n, \infty[$. In particular, the function υ_n is oscillating.*

We are now prepared to understand the rate of attenuation of the reduced energy function E_n.

Theorem 5 *The function*

$$r \mapsto \int_{A_n}^{r} \frac{\cos(2\varphi_n)}{\varrho}\mathrm{d}\varrho$$

has a limit at infinity.

Proof. Take a real number $r_1 > 0$ such that $\mathrm{d}\varphi_n/\mathrm{d}\varrho > 0$ for all $\varrho \geqslant r_1$; set

$$\psi_n(\varrho) = \varrho\frac{\mathrm{d}\varphi_n}{\mathrm{d}\varrho}.$$

Then for $r_2 > r_1$, an integration by parts yields

$$\int_{r_1}^{r_2} \frac{\cos(2\varphi_n)}{\varrho}\mathrm{d}\varrho = \left[\frac{\sin(2\varphi_n)}{2\psi_n}\right]_{r_1}^{r_2} + \int_{r}^{R} \frac{\mathrm{d}\psi_n}{\mathrm{d}\varrho}\frac{\sin(2\varphi_n)}{2\psi_n^2}\mathrm{d}\varrho.$$

The first term of the right hand side behaves as follows

$$\lim_{r_2\to\infty}\left[\frac{\sin(2\varphi_n)}{2\psi_n}\right]_{r_1}^{r_2} = -\frac{\sin(2\varphi_n)}{2\psi_n(r_1)}.$$

The second term may be dealt with by observing that

$$\begin{aligned}\frac{\mathrm{d}\psi_n}{\mathrm{d}\varrho} &= H(n+2)\varrho^{n/2}(1-2\cos(2\varphi_n))\cosh\upsilon_n \\ &\quad + \frac{(n+2)^2}{4\varrho}\sin(4\varphi_n) - \varrho^{n+1}E_n\sin(2\varphi_n),\end{aligned}$$

from which we deduce

$$\begin{aligned}\frac{1+o\left(1\right)}{2\psi_n^2}\frac{\mathrm{d}\psi_n}{\mathrm{d}\varrho} &= \frac{n+2}{2H}\frac{1-2\cos\left(2\varphi_n\right)}{\varrho^{n/2+2}}\cosh\upsilon_n \\ &\quad + \left(\frac{n+2}{2H}\right)^2\frac{\sin\left(4\varphi_n\right)}{2\varrho^{n+3}} - \frac{\sin\left(2\varphi_n\right)}{2H^2}\frac{E_n}{\varrho} \\ &= -\frac{\sin\left(2\varphi_n\right)}{2H^2}\frac{E_n}{\varrho} + \mathcal{O}\left(\frac{1}{\varrho^2}\right).\end{aligned}$$

Then, it is easily seen that the limit

$$\lim_{r_2\to\infty}\int_{r1}^{r_2}\frac{\mathrm{d}\psi_n}{\mathrm{d}\varrho}\frac{\sin\left(2\varphi_n\right)}{2\psi_n^2}\mathrm{d}\varrho$$

exists; the claim then follows at once. □

We arrive at the key estimation of this section:

Theorem 6 *There exists a positive real number A such that*

$$\lim_{\varrho\to\infty}\varrho^{1+\frac{n}{2}}E_n\left(\varrho\right) = A.$$

Proof. By definition — equation (16) — we have

$$E_n\left(r_2\right) = E_n\left(r_1\right)\exp\int_{r_1}^{r_2}\alpha_n,$$

for $r_2 > r_1$ and r_1 large enough. But then equation (18) yields

$$\begin{aligned}\int_{r_1}^{r_2}\alpha_n &= -\int_{r_1}^{r_2}\frac{n+2}{2\varrho}\left(1-\cos\left(2\varphi_n\right)\right)\mathrm{d}\varrho \\ &= -\frac{n+2}{2}\ln\frac{r_2}{r_1} + \frac{n+2}{2}\int_{r_1}^{r_2}\frac{\cos\left(2\varphi_n\right)}{\varrho}\mathrm{d}\varrho.\end{aligned}$$

And theorem 5 asserts that the second term of the right hand side has a finit value as r_2 goes to infinity. □

Theorem 7 *For all positive real number a, the limits of the functions*

$$r \mapsto \int_{A_n}^{r} \frac{E_n}{\varrho} \quad \textit{and} \quad r \mapsto \int_{A_n}^{r} \frac{\cos 2\varphi_n}{\varrho^a}$$

exist as r approches infinity.

7 Symmetries

In this section, we establish the existence of extrinsic reflectional symmetries of Smyth surfaces. We begin with the following properties of the radial lines through the umbilical point: The curves $\vartheta = \mathrm{const}$ are geodesic curves on a smyth surface. That follows at once from the formula (4). Next, we have the following geometric facts:

Proposition 1 *The curves $\vartheta = k\pi/(n+2)$ drawn on a Smyth surface of order n are planar curvature lines, congruent to each other through a rotation of angle $\pi/(n+2)$ about the normal at the umbilical point.*

Proof. We may first observe that such a curve is a line of curvature. Since it is also a geodesic, it is planar and its containing plane is orthogonal to Smyth_n. Since the immersion is conformal, it preserves angles between the defining curves at the umbilical point. □

The two geometric properties shown above may be summarized in the following:

Theorem 8 *Any Smyth surface of order $n \in \mathbb{N}$ admits $n+2$ plans of symmetry, meeting along a normal line at the umbilical point.*

We would like to emphasize how the geometry of the Hopf differential, coupled with an intrinsic symmetry, gives rise to extrinsic symmetries. Those symmetries will be used to reduce the numerical construction of a Smyth surface to an angular sector of measure $\pi/(n+2)$.

8 The Geometry of the legs

The planar curves characterized in proposition 1 are the curves along which the chordal-distance function $\mathrm{chord}\,(z) = \|\mathbf{Sm}_n\,(z) - \mathbf{Sm}_n\,(0)\|$ from the umbilic to an arbitrary point on $\mathbf{Sm}_n$grows the fastest or the slowest. Such curves are called the legs of $\mathbf{Sm}_n$. They are images by rigid motions of the two planar curves $\boldsymbol{\gamma}_n^+ = \mathbf{Sm}_n\,(\cdot,\,0)$ and $\boldsymbol{\gamma}_n^- = \mathbf{Sm}_n\,(\cdot,\,\pi/(n+2))$. To fix the ideas, we consider the instance of $\mathbf{Sm}_n$that satisfies the initial conditions

$$\mathbf{Sm}_n\,(0) = O \in \mathcal{E}^3, \quad \left.\frac{\partial \mathbf{Sm}_n}{\partial \varrho}\right|_{\varrho=0} = \frac{\sigma}{H}\begin{pmatrix}1\\0\\0\end{pmatrix} \quad \text{and} \quad \boldsymbol{N}_n\,(0) = \begin{pmatrix}0\\0\\1\end{pmatrix}.$$

The curves $\boldsymbol{\gamma}_n^+$ and $\boldsymbol{\gamma}_n^-$ are defined by the differential relations

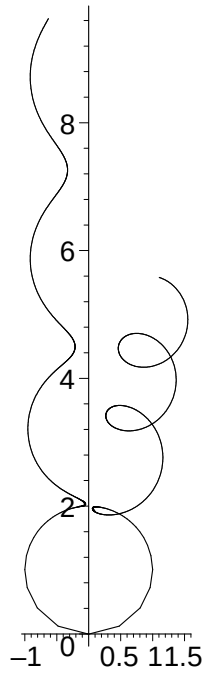

Figure 3: Planar curvature lines for $\sigma = 100$ and $n = 1$

$$\begin{cases} \dfrac{\mathrm{d}^2\boldsymbol{\gamma}_n^+}{\mathrm{d}\varrho^2} = \dfrac{\mathrm{d}\omega}{\mathrm{d}\varrho}\dfrac{\mathrm{d}\boldsymbol{\gamma}_n^+}{\mathrm{d}\varrho} + H\left(\mathrm{e}^{2\omega} + \varrho^n\right)\boldsymbol{N}_n^+ \\ \dfrac{\mathrm{d}\boldsymbol{N}_n^+}{\mathrm{d}\varrho} = -H\left(1 + \varrho^n\,\mathrm{e}^{-2\omega}\right)\dfrac{\mathrm{d}\boldsymbol{\gamma}_n^+}{\mathrm{d}\varrho} \end{cases}, \quad \left.\frac{\mathrm{d}\boldsymbol{\gamma}_n^+}{\mathrm{d}\varrho}\right|_{\varrho=0} = \frac{\sigma}{H}\begin{pmatrix}1\\0\\0\end{pmatrix} \tag{20}$$

and

$$\begin{cases} \dfrac{\mathrm{d}^2\boldsymbol{\gamma}_n^-}{\mathrm{d}\varrho^2} = \dfrac{\mathrm{d}\omega}{\mathrm{d}\varrho}\dfrac{\mathrm{d}\boldsymbol{\gamma}_n^-}{\mathrm{d}\varrho} + H\left(\mathrm{e}^{2\omega} - \varrho^n\right)\boldsymbol{N}_n^- \\ \dfrac{\mathrm{d}\boldsymbol{N}_n^-}{\mathrm{d}\varrho} = -H\left(1 - \varrho^n\,\mathrm{e}^{-2\omega}\right)\dfrac{\mathrm{d}\boldsymbol{\gamma}_n^-}{\mathrm{d}\varrho} \end{cases}, \quad \left.\frac{\mathrm{d}\boldsymbol{\gamma}_n^-}{\mathrm{d}\varrho}\right|_{\varrho=0} = \frac{-\sigma}{H}\begin{pmatrix}1\\0\\0\end{pmatrix}. \tag{21}$$

For a fixed mean curvature H, the value of the parameter σ is the magnitude of the initial speed of the geodesics γ_n^+ and γ_n^-.

Proposition 2 *The curvature of the planar curves $\boldsymbol{\gamma}_n^+$ and $\boldsymbol{\gamma}_n^-$ tend to $2H$ and zero respectively as one goes to infinity.*

Proof. These are direct consequences of the estimations (15). We will give the proof for thr curve $\boldsymbol{\gamma}_n^+$; that proof for $\boldsymbol{\gamma}_n^-$ is similar. If we denote by ψ a differentiable determination of the angle between the running tangent vector $\mathrm{d}\boldsymbol{\gamma}_n^+/\mathrm{d}\varrho$ and the initial direction, then we know the curvature of $\boldsymbol{\gamma}_n^+$ is given by the expression

$$\kappa^+ = \frac{\mathrm{d}\psi}{\mathrm{d}s} = \frac{\mathrm{d}\psi}{\mathrm{d}\varrho}\frac{\mathrm{d}\varrho}{\mathrm{d}s} = H\left(1 + \varrho^n\,\mathrm{e}^{-2\omega}\right)$$

where s is the arclength parameter along $\boldsymbol{\gamma}_n^+$. Hence the claim. □

9 Numerical constructions

The algorithm for effective (numerical) construction of a surface $\mathbf{Sm}_n$is based on the fundamental theorem of the theory of submanifold. Let us recall that the vector position and the normal are subject to the following systems of

partial differential equations (Gauss and Weingarten equations) written in polar coordinates

$$\begin{cases} \dfrac{\partial^2 \mathbf{Sm}_n}{\partial \varrho^2} = \dfrac{\mathrm{d}\omega_n}{\mathrm{d}\varrho}\dfrac{\partial \mathbf{Sm}_n}{\partial \varrho} + H\left[\mathrm{e}^{2\omega_n} + \varrho^n \cos(n+2)\,\vartheta\right]\boldsymbol{N}_n \\ \dfrac{1}{\varrho}\dfrac{\partial^2 \mathbf{Sm}_n}{\partial \varrho \partial \vartheta} = \left(\dfrac{1}{\varrho} + \dfrac{\mathrm{d}\omega_n}{\mathrm{d}\varrho}\right)\dfrac{1}{\varrho}\dfrac{\partial \mathbf{Sm}_n}{\partial \vartheta} - H\varrho^n \sin(n+2)\,\vartheta \boldsymbol{N}_n \\ \dfrac{1}{\varrho^2}\dfrac{\partial^2 \mathbf{Sm}_n}{\partial \vartheta^2} = -\left(\dfrac{1}{\varrho} + \dfrac{\mathrm{d}\omega_n}{\mathrm{d}\varrho}\right)\dfrac{\partial \mathbf{Sm}_n}{\partial \varrho} + H\left[\mathrm{e}^{2\omega_n} - \varrho^n \cos(n+2)\,\vartheta\right]\boldsymbol{N}_n \end{cases} \tag{22}$$

$$\begin{cases} \dfrac{1}{H}\dfrac{\partial \boldsymbol{N}_n}{\partial \varrho} = -\left[1 + \dfrac{\varrho^n}{\mathrm{e}^{2\omega}}\cos(n+2)\,\vartheta\right]\dfrac{\partial \mathbf{Sm}_n}{\partial \varrho} + \dfrac{\varrho^{n-1}}{\mathrm{e}^{2\omega}}\sin(n+2)\,\vartheta\dfrac{\partial \mathbf{Sm}_n}{\partial \vartheta} \\ \dfrac{1}{H\varrho}\dfrac{\partial \boldsymbol{N}_n}{\partial \vartheta} = \dfrac{\varrho^n}{\mathrm{e}^{2\omega}}\sin(n+2)\,\vartheta\dfrac{\partial \mathbf{Sm}_n}{\partial \varrho} - \left[1 - \dfrac{\varrho^n}{\mathrm{e}^{2\omega}}\cos(n+2)\,\vartheta\right]\dfrac{1}{\varrho}\dfrac{\partial \mathbf{Sm}_n}{\partial \vartheta} \end{cases}. \tag{23}$$

In general, there is no *a priori* reasons why systems of PDEs should have solutions. They ought to satisfy compatibility conditions. In our cases, those integrability equations are preciely the Mainardi–Codazzi and Gauss–Codazzi equations. As we have seen in section §3, the Mainardi–Codazzi equations express the holomorphic character of the associated Hopf differential, which is already folded in the above systems. The Gauss–Codazi equation is the differential equation that defines ω_n.

Concretely, the algorithm proceeds as follows:

1. Integrate the ODE (7);
2. Compute the functions $\mathbf{Sm}_n$and $\boldsymbol{N}_n$ — with their first partial derivates — along the planar curvature line defined by $\vartheta = 0$ by integrating ODE (20).
3. For fixed ϱ, integrate (for ϑ) the systems (22) and (23).

Some of the above steps may be conducted synchronously. Although we use a Runge–Kutta solver to integrate the ODEs appearing in the algorithm, any other ODE solver allowing a single step derivation is equally admissible. Here is a folded version of the algorithm:

Input $\sigma > 0$, $n \in \mathbb{N}$ and $\varrho_{\max} > 0$.

Output $\mathbf{Sm}_n(\varrho, , \vartheta)$ with $\varrho \in [0,\ \varrho_{\max}]$ and $\vartheta \in [0,\ 2\pi]$.

Body 1. Set initial conditions:

$$\mathbf{Sm}_n(0) = \begin{pmatrix} 0 \\ 0 \\ 0 \end{pmatrix}, \quad \left.\frac{\partial \mathbf{Sm}_n}{\partial \varrho}\right|_{\varrho=0} = \frac{\sigma}{H}\begin{pmatrix} 1 \\ 0 \\ 0 \end{pmatrix}, \quad \boldsymbol{N}_n(0) = \begin{pmatrix} 0 \\ 0 \\ 1 \end{pmatrix},$$
$$\omega_n(0) = \ln\frac{\sigma}{H}, \quad \left.\frac{\mathrm{d}\omega_n}{\mathrm{d}\varrho}\right|_{\varrho=0} = 0.$$

2. For ϑ in $[0,\ 2\pi]$, set

$$\mathbf{Sm}_n(0,\ \vartheta) = \begin{pmatrix} 0 \\ 0 \\ 0 \end{pmatrix}.$$

This corresponds to the fact that the curve $\varrho = 0$ is reduced to the umbilic point.

3. For ϱ running over $]0,\ \varrho_{\max}]$ do:
   - compute both the values $(\omega_n, \mathrm{d}\omega_n/\mathrm{d}\varrho)$ and the point $\boldsymbol{\gamma}_n^+(\varrho) = \mathbf{Sm}_n(\varrho,\ 0)$ by performing a Runge-Kutta step of the ODE systems (7) and (20).
   - For the above fixed ϱ, compute the ϑ-curve $\mathbf{Sm}_n(\varrho,\ \vartheta)$ for ϑ running over $[0,\ 2\pi]$ by solving the PDE systems (22) and (23).
4. Output the surface $\mathbf{Sm}_n$.

10 conclusion

The effective numerical algorithm exposed in this article has enabled us to gain highly invaluable insights into the geometry of Smyth surfaces. For example, numerical experiments suggest that the legs form an angle (see figure 3) function only of the parameter σ. The detailed invesgitation of that

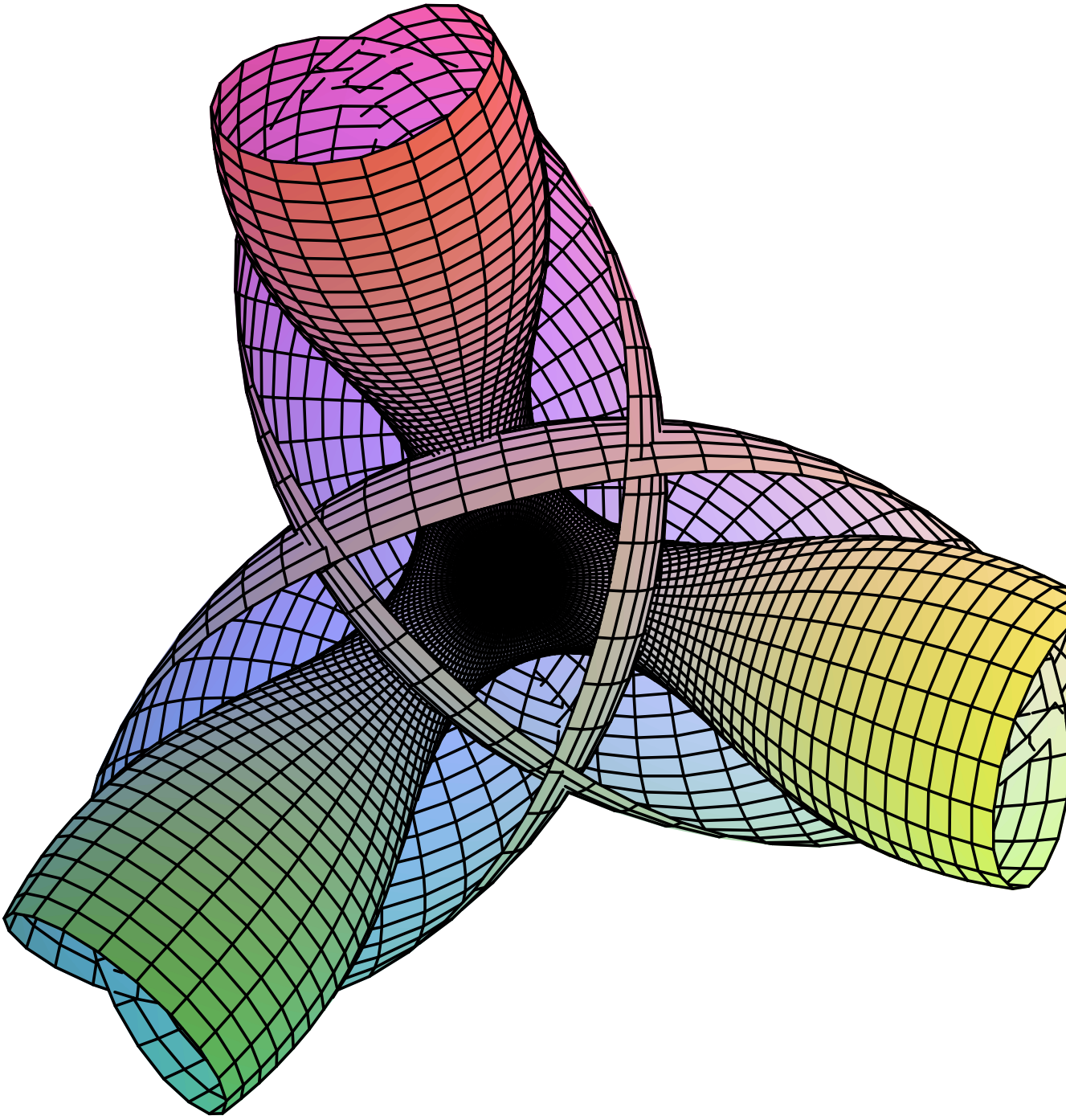

Figure 4: A Smyth surface for $n = 1$, view from "below"

behavior will be the subject of a forthcoming article based on algebraic and numerical analysis of the ODE (7). The generalization of some of the methods used here to the case where no *a priori* symmetry assumption is made on the metric (but retaining a monomial Hopf differential) is also under investigation.

References

[1] U. Abresch, *Constant Mean Curvature Tori In Terms Of Elliptic Functions*, J. reine und ang. Math. **374** (1987), 169–192.

[2] M.S. Baouendi and C. Goulaouic, *Singular nonlinear Cauchy problems*, Journal of Differential Equations **22** (1976), 268–321.

[3] A.I. Bobenko, *All constant mean curvature tori in $\mathbb{R}^3$, $\mathcal{S}^3$, $\mathcal{H}^3$ in terms of theta-functions*, Math. Ann. (1991), 209–245.

[4] ———, *Constant mean curvature surfaces and integrable equations*, Russian Mathematical Surveys **46** (1991), no. 4, 1–45.

[5] G. Darboux, *Leçons sur la théorie générale des surfaces*, Éditions Jacques Gabay, 1993.

[6] Ch. Delaunay, *Sur la surface de révolution dont la courbure moyenne est constante*, J. Math. P. Appl. **6** (1841), 309–320.

[7] J. Dorfmeister, F. Pedit, and H. Wu, *Weierstrass type representation of harmonic maps into symmetric spaces*, Comm. in Anal. Geom. **6** (1998), no. 4, 633–668.

[8] G. Dos Reis, *Sur les surfaces dont la courbure moyenne est constante*, Ph.D. thesis, Université Paris VII, 2001.

[9] ———, *Asymptotics of CMC surfaces with polynomial Hopf differential*, Calculus of Variations (to appear.).

[10] I. Kuzin and S. Pohozaef, *Entire Solutions of Semilinear Elliptic Equations*, Progress in Nonlinear Differential Equations and Their Applications, vol. 33, Birkhäuser, 1997.

[11] Olli Lehto, *Univalent Functions and Teichmüller Spaces*, Graduate Texts in Mathematics, no. 109, Springer-Verlag New York Inc., 1987.

[12] U. Pinkall and I. Sterling, *On the classification of constant mean curvature tori*, Ann. Math. **130** (1989), 407–451.

[13] B. Smyth, *A generalisation of a theorem of Delaunay on constant mean curvature surfaces*, Statistical Thermodynamics and Differential Geometry of Microstructured Material (H. Ted Davis and Johannes C.C. Nitsche, eds.), The IMA volumes in Mathematics and its applications, vol. 51, Springer-Verlag, 1993, pp. 123–130.

[14] M. Timmreck, U. Pinkall, and D. Ferus, *Constant mean curvature planes with inner rotational symmetry in Euclidan* 3*-space*, Mathematische Zeitschrift **215** (1994), 561–568.

[15] Henry C. Wente, *Conterexample to a Conjecture of H. Hopf*, Pacific J. of Math **121** (1986), 193–243.

Unité de recherche INRIA Sophia Antipolis
2004, route des Lucioles - BP 93 - 06902 Sophia Antipolis Cedex (France)

Unité de recherche INRIA Lorraine : LORIA, Technopôle de Nancy-Brabois - Campus scientifique
615, rue du Jardin Botanique - BP 101 - 54602 Villers-lès-Nancy Cedex (France)
Unité de recherche INRIA Rennes : IRISA, Campus universitaire de Beaulieu - 35042 Rennes Cedex (France)
Unité de recherche INRIA Rhône-Alpes : 655, avenue de l'Europe - 38330 Montbonnot-St-Martin (France)
Unité de recherche INRIA Rocquencourt : Domaine de Voluceau - Rocquencourt - BP 105 - 78153 Le Chesnay Cedex (France)

Éditeur
INRIA - Domaine de Voluceau - Rocquencourt, BP 105 - 78153 Le Chesnay Cedex (France)
http://www.inria.fr
ISSN 0249-6399